PREDICTION OF STRUCTURAL RESPONSE AND GROUND MOTION USING DEEP NEURAL NETWORKS

Issac Kwok-Tai Pang, Selim Günay, and Khalid M. Mosalam
University of California, Berkeley

Abstract

This paper presents a methodology to determine the time history of the structural response using the Temporal Convolutional Network (TCN), a deep learning method. The methodology, in conjunction with sensor data from instrumented buildings, facilitates the prediction of the response in future earthquakes without a structural analysis model, providing a computationally effective complement, or even alternative, to nonlinear time history analysis. The developed TCN model is applied for predicting the responses of numerical models, a shaking table tested structure, and instrumented buildings for a broad range of response characteristics. Furthermore, ground motions are predicted from the response accelerations using the TCN model. It is observed that the method successful predicted these responses using a practical number of recorded signals for training. The limitations of the adopted methodology are identified, which can be resolved in future studies with physics-informed AI methodologies.

Introduction

This paper aims at developing a methodology to determine the time history of the structural response using a deep learning approach, namely the Temporal Convolutional Network (TCN). When the developed methodology is adopted in conjunction with sensor data from instrumented buildings, it facilitates the prediction of the response in future earthquakes without structural analysis models. Accordingly, the adopted methodology complements or even provides a computationally effective alternative to nonlinear time history analysis.

There has been a limited number of studies in the literature to predict the structural response in the form of time histories using deep learning approaches. Some of these studies focused on only predicting the peak response (Zhong et al., 2023). Although the peak response is important in design, assessment, and Performance-Based Earthquake Engineering (PBEE), the entire response history provides a complete description of the structural behavior. One particular use of the entire response history is detection of the existence, severity, and location of damage in Structural Health Monitoring (SHM), where the peak response is generally insufficient for this purpose (Muin and Mosalam, 2017, 2018; Park and Ang, 1985, Park et al., 1985). Therefore, there has been some studies focused on predicting the entire response using machine learning (e.g., Chen et al., 2023; Zhang et al., 2019; Kundu and Chakraborty, 2020; Li and Spence, 2020). In these studies, either a structural component or a single instrumented building was considered without providing detailed physical explanations of the data-driven predictions.

The developed TCN model herein is applied to predict the time history of the structural response of systems with various characteristics as outlined in Table 1. These characteristics include elastic and inelastic response, single mode and higher modes of vibration, and constant and varying damping ratios. The dynamic responses of these systems are characterized by the listed features in Table 1. Successful response predictions of the TCN model require the learning and accurate characterization of these features with varying complexities, as discussed in the following sections. The accuracy and challenges of the predictions for each system are discussed using concepts from structural dynamics. In addition to these predictions, reverse engineering is adopted for predictions of ground motions from measured or computed response accelerations.

Table 1.	Features	characterizing	the earthqui	ake response of	f different structural	systems

Response	System	Feature 1	Feature 2	Feature 3
	SDOF*	Natural period	Damping ratio	Ground motion
Linear elastic	Low- and Mid-rise Buildings	First mode period	Varying first mode damping ratios	
elastic	Tall Buildings	Periods for multiple modes	Damping ratios of multiple modes	motion
Inelastic	SDOF	Natural period & damping ratio	Force capacity	Ground
inerasuc	Low and Mid-rise Buildings	Elongation of first mode period	Varying first mode damping ratio	motion

^{*}Single Degree Of Freedom

Temporal Convolutional Network

The TCN was proposed by Lea et al. (2017) and is a powerful and innovative deep learning architecture designed for processing sequential data, particularly for time-series analysis and natural language processing tasks, refer to Figure 1. TCNs are built upon the Convolutional Neural Networks (CNNs), but they can be adapted to model temporal dependencies in sequential data, making them suitable for tasks which require understanding patterns and trends over time. TCNs employ a stack of one-dimensional convolutional layers to efficiently learn dependencies across different time steps. This design allows TCNs to utilize parallel computing, which makes them efficient and fast to train. TCNs have gained popularity due to their ability to capture long-range dependencies in sequential data without suffering from the vanishing gradient problem often encountered by other deep learning methods, like Recurrent Neural Networks (RNNs). They have been successfully applied in various domains, such as natural language processing, speech recognition, and sensor data analysis.

SDOF Numerical Model

For verification of the developed TCN model and its implementation, the acceleration responses of a linear elastic SDOF system are predicted and compared with the computed results. For this purpose, a SDOF system is considered (period = 0.41 sec and damping ratio = 2.35%). It is trained using 11 motions and tested using 7 motions. The chosen period and damping ratio are those identified for the San Bernardino 6-story hotel in the NS direction, which is discussed in the next section. The motions used for training and testing are the recorded ground and response accelerations of the same hotel building. The predictions are very accurate with a correlation

coefficient of 99.99% over the 7 tested motions, verifying the implementation of the TCN method. The predicted acceleration time histories are compared with the computed ones (referred to as real) for one of the test motions (Fontana Earthquake of 25 July 2015) in Figure 2, along with the comparison of the frequency contents, showing a very close match.

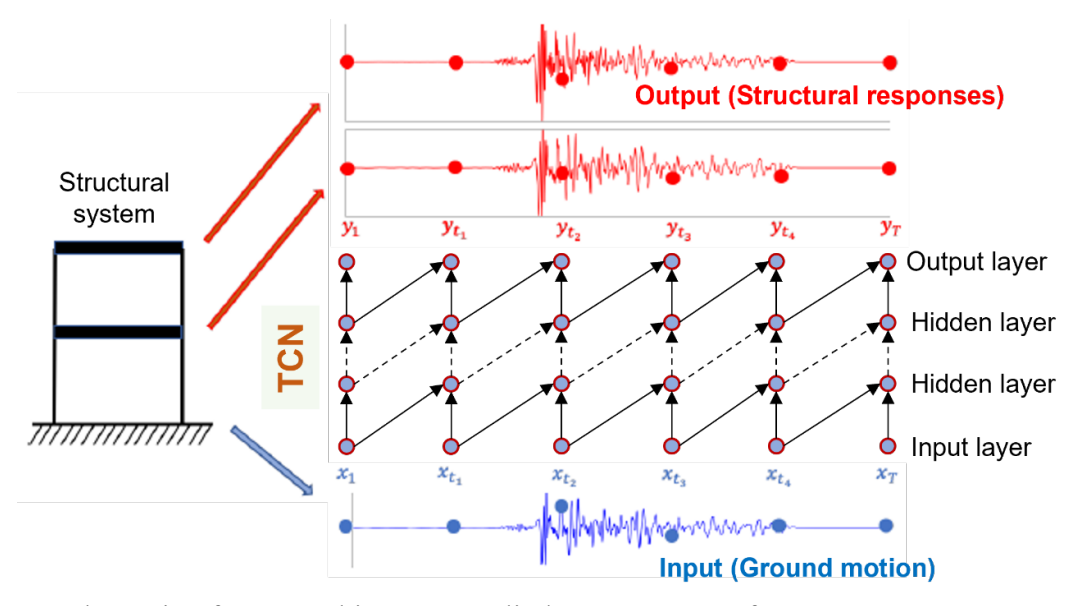


Figure 1. Schematic of TCN architecture applied to a two-story frame.

Linear Elastic Response Prediction

The response of an elastic SDOF system subjected to ground motions depends only on: (a) the natural period of the SDOF system, (b) the damping ratio of the SDOF system, and (c) the applied ground motion (Table 1). The highly accurate predictions of the SDOF system indicate that the TCN model is successful in learning the period and the damping ratio (Features 1 and 2, respectively, in Table 1) and the training model has enough variety of the ground motions for the model to learn the SDOF response when subjected to different excitations (Feature 3 in Table 1).

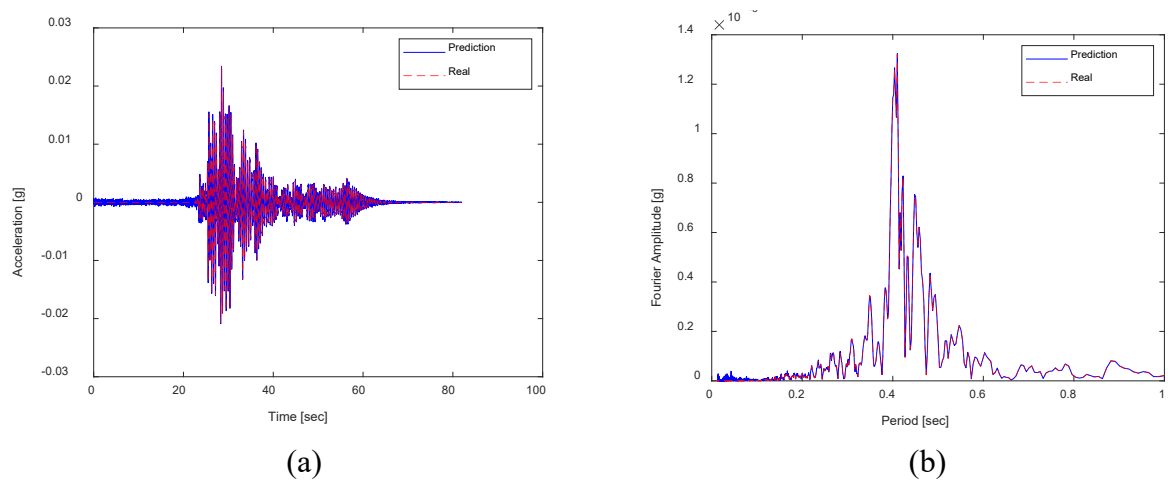


Figure 2. Comparison of (a) time history, (b) frequency contents of the predicted and computed acceleration of the linear elastic SDOF system in Fontana Earthquake of 25 July 2015.

6-Story Reinforced Concrete (RC) Hotel Building in San Bernardino EW Direction

Predictions are performed for the linear elastic response of two instrumented CSMIP buildings. One of them is discussed, namely, the 6-story RC Shear Wall (RCSW) hotel building in San Bernardino, California, designed in 1970 (Figure 3). This building is instrumented with 9 accelerometers, three on each of the 1st, 3rd, and 6th (roof) floors, and has recorded multiple seismic events from 1987 to 2018. The EW and NS direction responses of this building are studied in this section for the linear response and in a later section for the inelastic response. In the EW direction, Channel 1 on the 1st floor is used as input, and Channels 4 and 7, on the 3rd floor and roof, respectively, are used as outputs. It is noted that the 1st floor boundary conditions are fixed. Therefore, Channel 1 directly represents the ground motion input to the structure. There are a total of 26 events recorded by this station, and 11 and 7 of these records are respectively used for training and testing. As shown in Figure 4, the motions used in the training set cover the entire range of shaking levels recorded on this building. It is possible to use another Intensity Measure (IM) to define the horizontal axis of this figure. However, the Peak Ground Acceleration (PGA) is used for simplicity as the objective is not to use the IM for quantitative damage detection, but it is rather used to graphically characterize the training and testing set motions as a function of the experienced shaking levels. Eleven motions were sufficient for predicting accurate results for the linear elastic response in the EW direction, and a larger number of motions were utilized for capturing the nonlinear response in the NS direction.

It is noted that unprocessed accelerations are used for all studied instrumented buildings. This is because the processed output is not necessarily the direct result of the processed ground motion input. Therefore, the relationship between the input and output deviates slightly from the true behavior when processed data is used for input and output. This explanation was also supported by the slightly higher accuracy of predictions with unprocessed accelerations as compared to processed accelerations (91% versus 88% in Table 2).

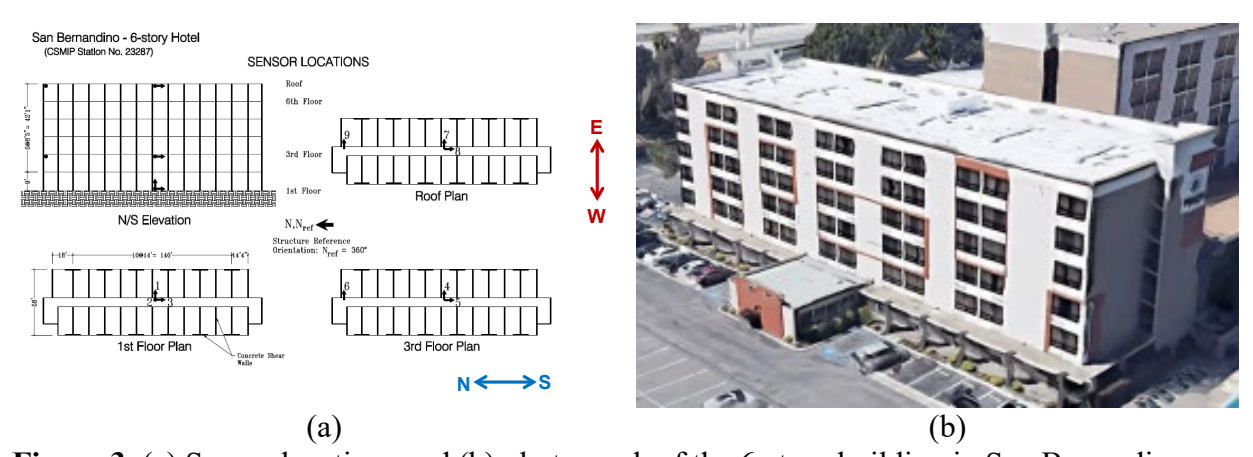


Figure 3. (a) Sensor locations and (b) photograph of the 6-story building in San Bernardino.

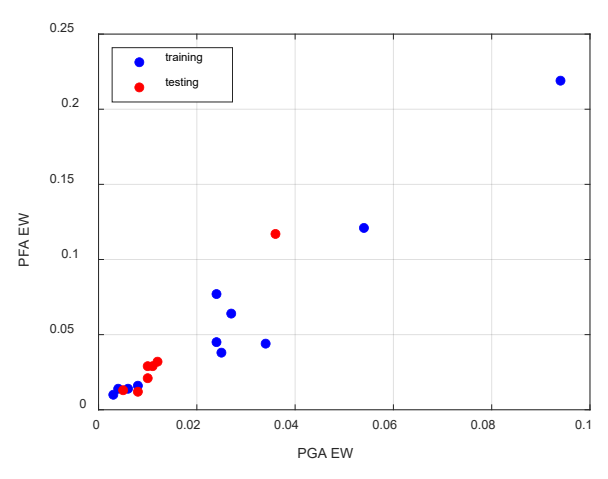


Figure 4. The training and testing sets used for San Bernardino 6-story building EW direction.

Table 2. Accuracy of San Bernardino 6-story building acceleration predictions in E-W direction.

Data	Correlation Coefficient			
Data	Training Set	Testing Set		
Unprocessed	0.97	0.91		
Processed	0.97	0.88		

The predicted acceleration time histories at the 3rd and 6th (roof) floors are compared with the recorded time histories for one of the test motions (Chino Hills Earthquake of 29 July 2008) in Figure 5. This is presented along with the comparison of the frequency contents, showing a close match at both floors in the time and frequency domains.

From a structural dynamics perspective, the linear elastic response of a Multi-Degree of Freedom (MDOF) system depends on the natural periods, damping ratios, and mode shapes. The response of low and mid-rise buildings is generally governed by the first mode, which is also the case for the San Bernardino 6-story hotel building. Therefore, similar to the previously discussed SDOF system, the features that define the response are the period and damping ratio of the first mode and the ground motion itself (Table 1). It is noted that the response also depends on the mode shape. However, the first mode shape and the modal participation factor can be considered as a constant scale factor for all motions and therefore the mode shape is not listed as a feature in Table 1 for this system.

Although all motions are in the linear elastic range as observed by the identified natural periods, damping ratios vary because of the contribution and complexity of different mechanisms to damping at different intensities (Figure 6). The phenomenon of varying damping levels in the linear elastic response is well-known (e.g., Chopra, 2012; Cruz and Miranda, 2017). Even for the same motion in forced vibrations or ambient conditions, the damping ratio varies from segment to segment of the motion (Brownjohn et al., 2018). For proper training, the number of motions in the training set should be sufficient and of different intensities to capture different levels of damping ratios. Therefore, a few motions are not sufficient for learning the damping ratio feature as opposed to the case for the period feature where more motions are needed in the training set to accurately predict the damping. The results of this case study indicated that 10 ground motions were sufficient to learn the period and damping features for consequent accurate predictions.

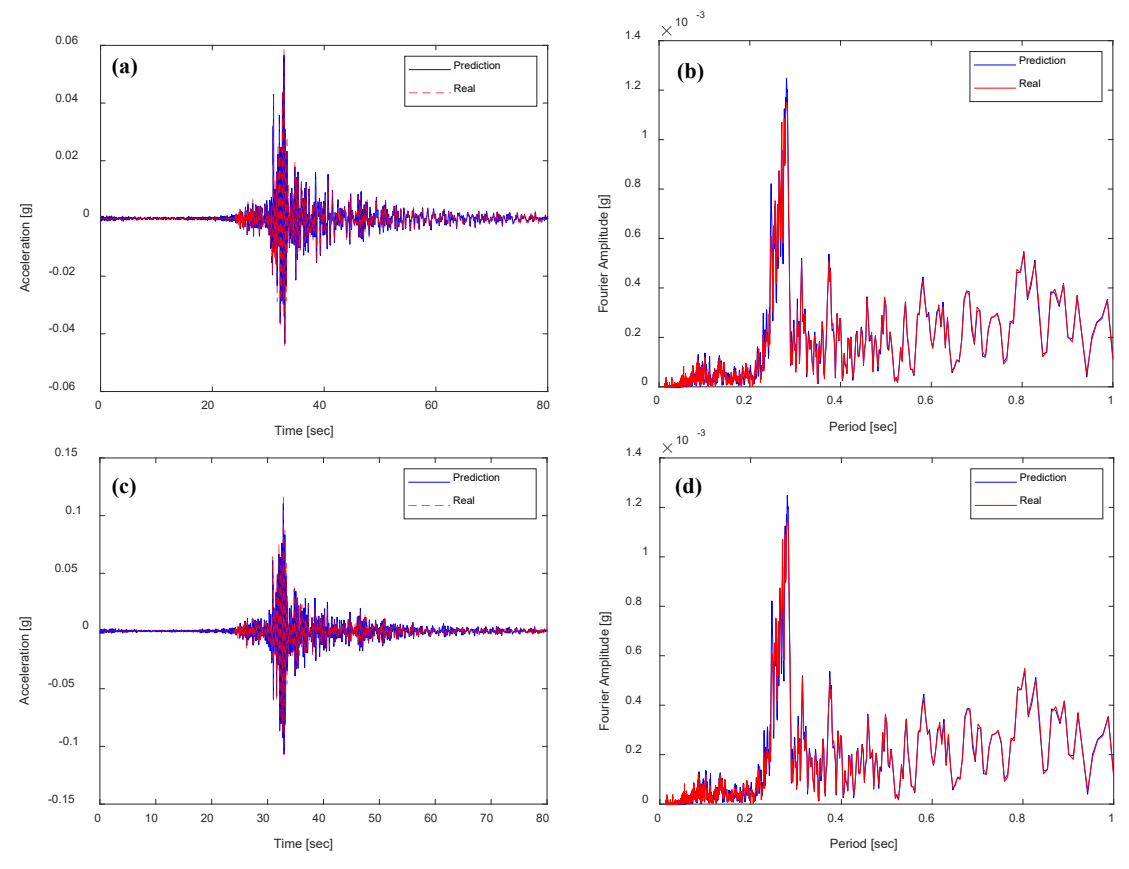


Figure 5. Comparison of predicted and recorded acceleration time history and the corresponding frequency contents in the EW direction of the San Bernardino 6-story building at (a, b) 3rd floor, (c, d) 6th floor (Chino Hills Earthquake of 29 July 2008).

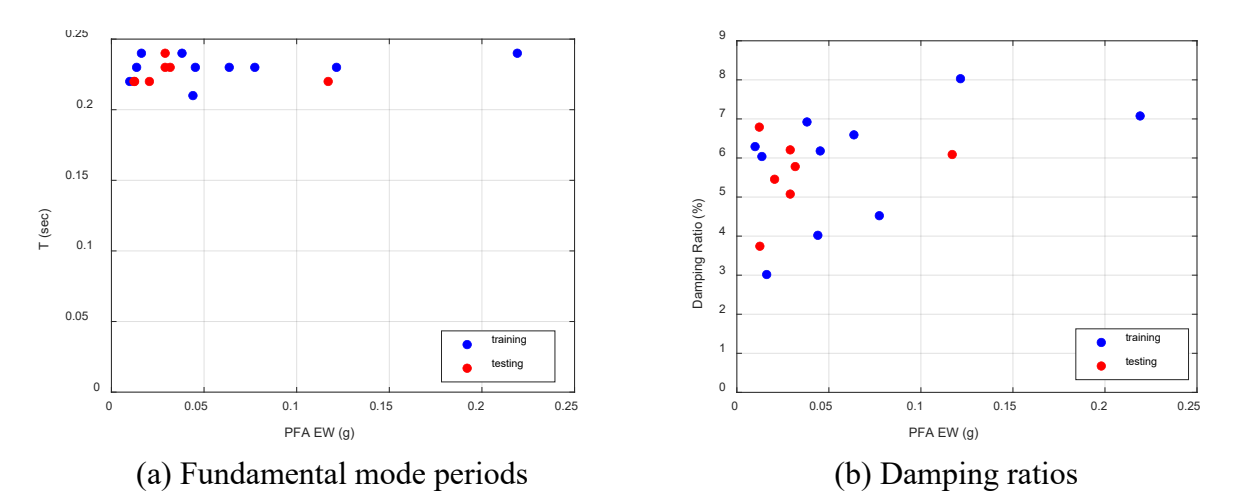


Figure 6. Identified features for San Bernardino 6-story building.

To demonstrate that accurate predictions are obtained for similar low- and mid-rise buildings with similar number of records in the training set, a 4-story hospital building in Hemet, California with RCSW structural system (similar to San Bernadino Hotel) is tested using the same TCN model. Accurate predictions were obtained using the same number of motions in the training set as the San Bernardino hotel building, i.e., 10 motions (Günay et al., 2023).

Tall Building with Higher Modes

Different from low-rise and mid-rise buildings, the seismic response of a tall building includes higher mode effects. From a structural dynamics perspective, the features that should be accurately characterized for a tall building are the periods and the damping ratios of several modes contributing to the response (Table 1). The response also depends on the mode shapes, however, as discussed earlier, the mode shape and the modal participation factor can be considered as a constant scale factor in the linear elastic dynamic response of each mode for each motion and accordingly is not considered as an explicit feature. Considering the increased number of features, the presence of multiple modes in the response may introduce additional challenges to the process of learning, impacting the accuracy of the predictions. Therefore, a 54story instrumented building is selected to explore the TCN predictions for a case where higher modes are clearly present in the response. This 54-story building is a Steel Moment Resisting Frame (SMRF) building with composite slabs of 2.5 inches thick concrete over 3 inches steel deck located in Los Angeles (LA), Figure 7. From this figure, the building is instrumented with 20 accelerometers at the basement (4 levels below ground), ground level, and the 20th, 36th, 46th and the penthouse floors. There are Vierendeel trusses and 48-inch-deep transfer girders at the 36th and 46th floors where vertical setbacks occur. Because there is a sudden change of stiffness at these locations, increased accelerations are expected, and sensors are placed at these floors for monitoring this expected increase of accelerations.

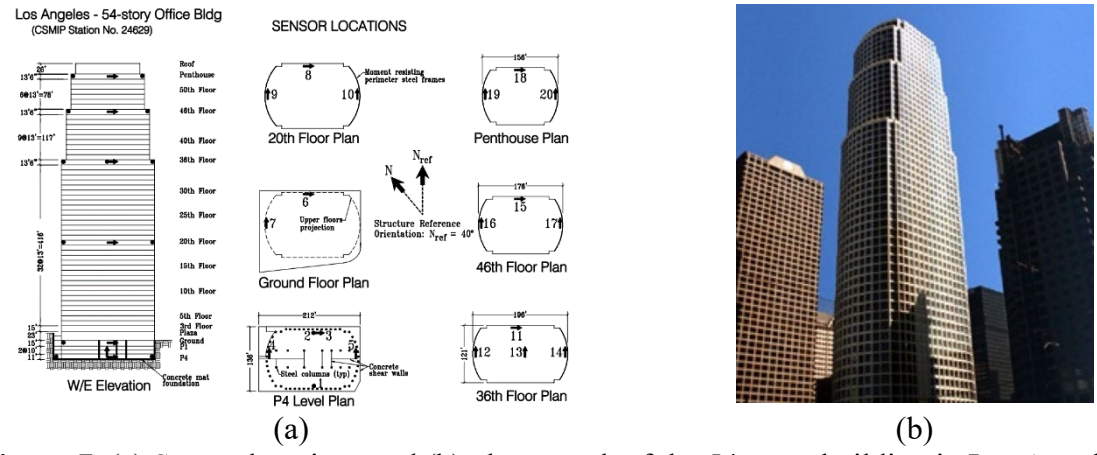


Figure 7. (a) Sensor locations and (b) photograph of the 54-story building in Los Angeles.

In this case study, which has 11 recorded motions, 10 motions are used for training and the remaining one motion is used for testing (Figure 8). The testing motion in the EW direction is particularly interesting as the Peak Floor Acceleration (PFA) is smaller than the corresponding PGA. This is attributed to: (a) the shape of the response spectrum for this motion, where the response acceleration at the first mode period of the building is smaller than the PGA, and (b) multiple modes counteracting and reducing the accelerations. The successful predictions in the EW and NS directions at the 46th floor for the considered test motion are shown in Figure 9. This figure demonstrates that the trained TCN model is successful in learning more complex responses obtained as a superposition of multiple modes and the 10-motion training set results in accurate responses as in the cases of San Bernardino and Hemet buildings.

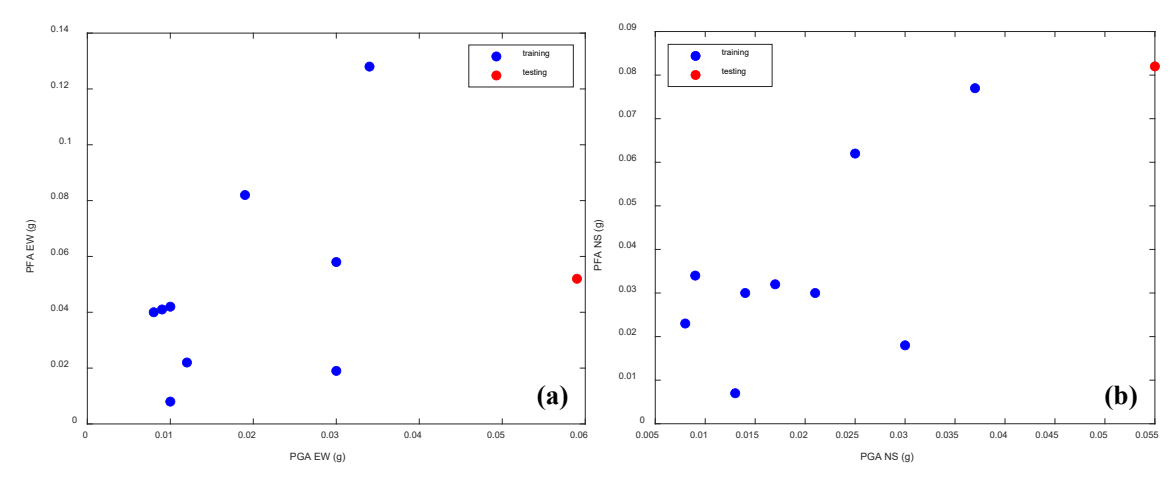


Figure 8. Training and testing sets used for LA 54 story building (a) EW, and (b) NS directions.

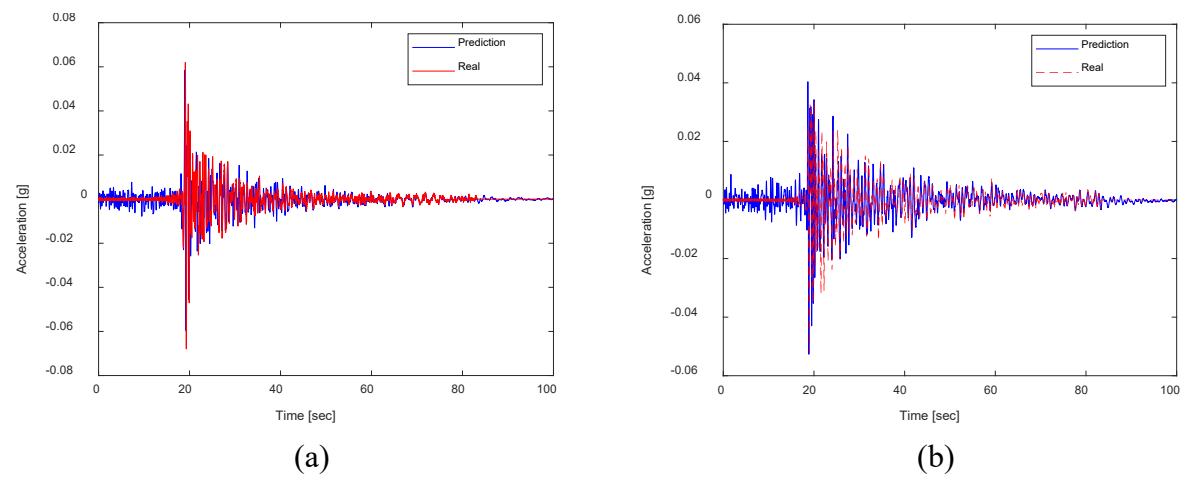


Figure 9. The 46th story acceleration predictions for the 56-story building in LA: (a) EW, and (b) NS directions (Chino Hills Earthquake of 29 July 2008).

Inelastic Response Prediction

As shown in Table 1, inelastic response predictions were conducted for a SDOF system, and low and mid-rise buildings, one of which is a three-story structure tested in the laboratory, while the other one is the NS direction of the San Bernardino 6-story building discussed before. The predictions of these three cases are discussed in the following sections.

6-Story RC Hotel Building in San Bernardino NS Direction

The identified periods of this building in the EW direction are almost constant in the tight range of 0.21 to 0.24 sec, independent of the level of shaking, which is indicative of linear elastic response (Figure 10a). On the other hand, the periods in the NS direction clearly increase with the level of shaking, indicating inelastic response (Figure 10b). Although it is not entirely clear why this period elongation occurred since the set of training ground motions is for low-level motions, possible reasons can be minor cracking, foundation rocking, disengagement of partition walls providing stiffness, or loss of contributions from other nonstructural components.

Although the inelastic response of this case study is not extensive, it presents a more challenging case for prediction compared to the linear elastic response. To predict the inelastic response in the NS direction, the same 10 motions used in the EW direction were not sufficient. As observed in Table 1, the features that need to be characterized for predicting the linear elastic and inelastic responses of a low- or mid-rise building is the first mode period and the first mode period elongation, respectively. The accurate characterization of period elongation requires not only a larger number of motions, but also the use of motions that span the entire range of period elongation. As mentioned earlier, the total number of events recorded for this building is 26. Out of these 26 motions, 23 ones covering the entire range of shaking levels were used for training as shown in Figure 11 and three events in the middle of the intensity range of these motions are used for testing. The results show the increased accuracy of the predictions as demonstrated in Figure 12 for one of the motions in the testing set. Particularly, the time history, the peaks, and the frequency contents are well matched, indicating that increasing the number of motions in the training set from 11 to 23 led to successful characterization of the increase of the period elongation with increased shaking intensity.

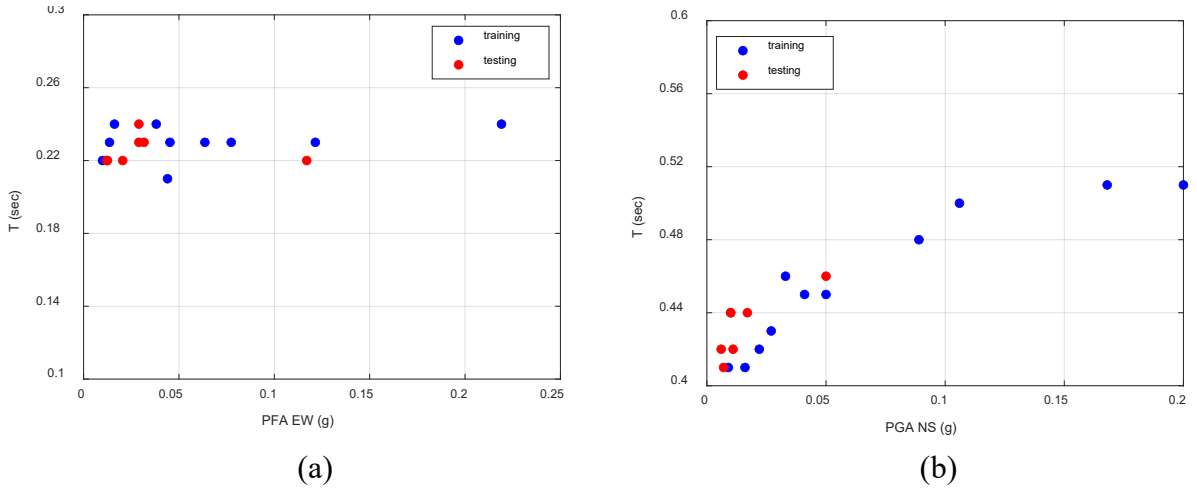


Figure 10. Identified periods of San Bernardino 6-story hotel building in (a) EW, and (b) NS directions in different earthquakes.

These successful predictions highlight an important and unique characteristic of obtaining the response using a deep learning approach. Several reasons cause the observed period elongation with increased intensity of shaking (e.g., concrete cracking, foundation rocking, and disengagement of partition walls, or loss of contributions from other nonstructural components). None of these aspects are considered explicitly in the computational models developed for structural dynamic analysis. Even if they are modeled, there are many sources of *epistemic* uncertainties associated with this type of modeling. Therefore, the obtained data-driven TCN model results show that the adopted deep learning approach fills this gap and results in accurate structural response prediction that would not be possible using conventional dynamic analysis. This case study also highlights two important aspects worthy of future investigation, namely, the effect of increased size of the training dataset (justifying need for more instrumented systems) and a hybrid use of physics-based and data-driven models where the data-driven model improves the predictions in cases where the physics-based modeling capabilities are insufficient.

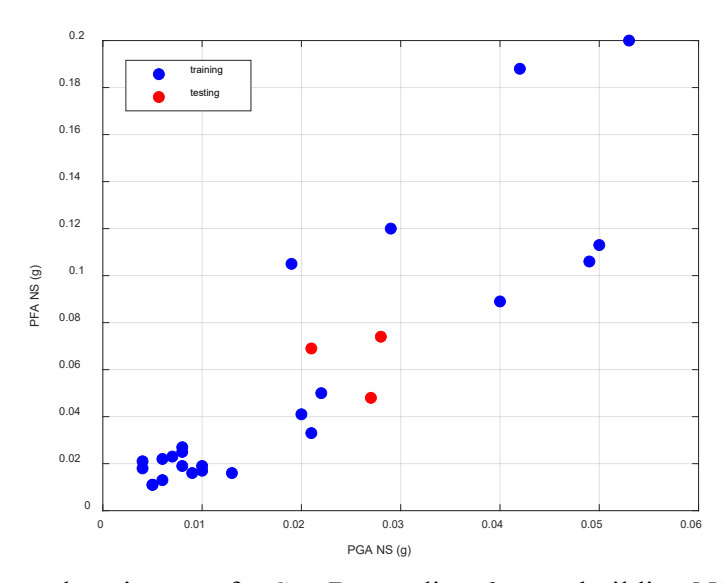


Figure 11. Training and testing sets for San Bernardino 6-story building NS direction.

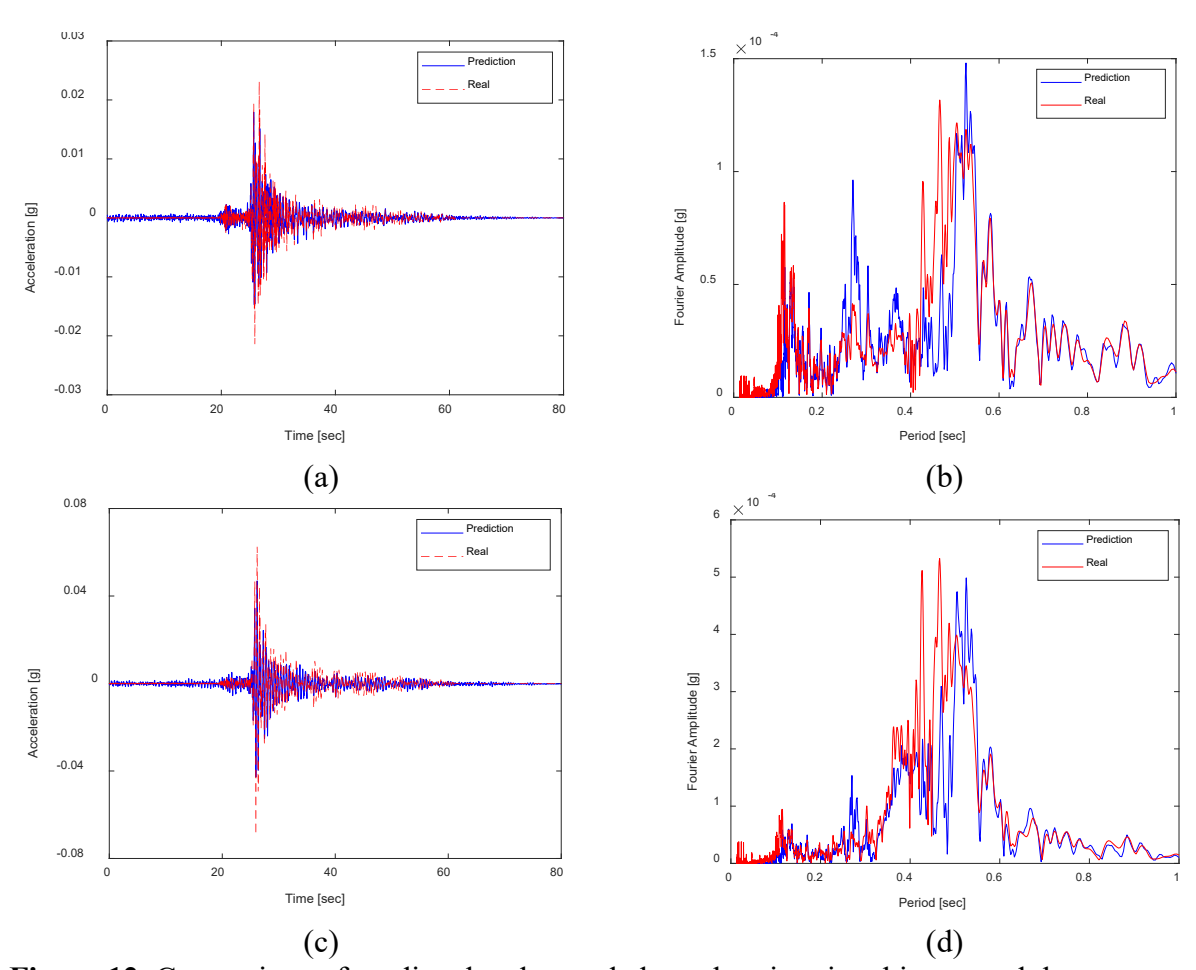


Figure 12. Comparison of predicted and recorded acceleration time history and the corresponding frequency contents in the NS direction of San Bernardino 6-story building at (a, b) 3rd floor, (c, d) 6th floor (Chino Hills Earthquake of 07 Aug. 2012).

Laboratory Testing of a 3-Story REPEAT Frame

Some instrumented buildings exist in the Center for Engineering Strong Motion Data (CESMD) database which experienced damage in previous earthquakes, e.g., the 7-story hotel in Van Nuys damaged in the 1994 Northridge earthquake. However, the number of earthquakes with inelastic response in these buildings is limited for meaningful training. Therefore, the results from a shaking table test are used as another system to predict its inelastic response.

The tested structure is a 3-story SMRF and was tested on the 6 Degree-of-Freedom (DOF) PEER (Pacific Earthquake Engineering Research) Center shaking table at UC-Berkeley. Test structure photographs are shown in Figure 13. The frame is assembled using steel beam-column elements, cross-joints, and clevises. The beams and columns are 65" long, 5"×5"×3/8" Hollow Square Section (HSS) members. There are 1" thick plates at each end of the members to attach them to the beam-column connections. The cross-joints at the connections are composed of the same HSS profile and plates.

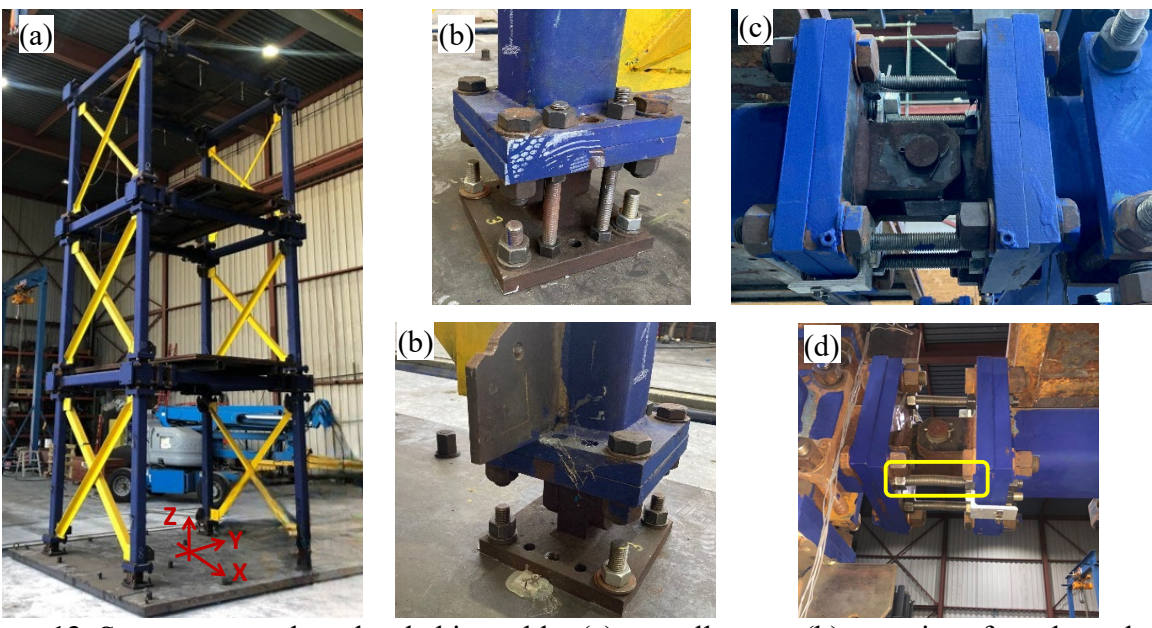


Figure 13. Structure tested on the shaking table: (a) overall setup, (b) two vies of a column base, (c) end beam connection, and (d) inelastic response in the form of coupon buckling.

The structure is tested along the Y-direction only by applying ground motions to the table. Along this direction, beams are connected to the cross-joints using clevises and coupons (Figure 13c), resulting in semi-rigid connections. The flexural stiffness of these connections is provided by a couple moment developed by the coupons. Following the principles of capacity design, the sizes and number of coupons are selected such that the capacity of this couple moment is smaller than the yield moment of the beam HSS section to protect the beams from yielding. Thus, the damage occurs only at the coupons (Figure 13d), which can be easily replaced, and the frame reconstructed conveniently each time after destructive testing (thus, the name REPEAT stands for REconfigurable Platform for EArthquake Testing). The columns are directly connected to the cross-joints resulting in rigid connections. Following principles of earthquake design, columns are designed to be stronger than beams, preventing the yielding of columns. There are two 3/4"

diameter threaded bars on the outside of each column clevis at the base (Figure 13b). Each beam-column joint has four of these threaded bars, two on each side of the clevis (Figure 13c).

The test matrix is shown in Table 3. Three ground motions are applied incrementally leading to linear elastic and inelastic response of the structure. Two of these motions are the ground motions recorded during the 1989 Loma Prieta earthquake. The third is a simulated ground motion obtained from physics-based simulations of the San Francisco Bay Area. In such simulations, a numerical model of the geologic and local soil layers is developed in a large area (e.g., the entire San Francisco Bay Area) and the ground motions at the earth's surface and subsurface are computed at closely spaced grid points. This is obtained from the numerical solution of the viscoelastic wave equation in both space and time initiated by a fault rupture model (McCallen et al., 2021). These simulated ground motions are validated against recorded ground motions in real earthquakes, and they are part of the PEER Center effort to develop a Simulated Ground Motion Database (SGMD), to be publicly available at the end of 2024.

Table 3. Test matrix used in the shaking table tests.

Run #	Ground Motion	Scale Factor	Run #	Ground Motion	Scale Factor
1	Simulated motion	0.25	10	Simulated motion	1.00
2	Loma Prieta Sunnyvale Station	0.25	11	Loma Prieta Sunnyvale Station	1.00
3	Loma Prieta Palo Alto Station	0.25	12	Loma Prieta Palo Alto Station	1.00
4	Simulated motion	0.50	13	Simulated motion	1.25
5	Loma Prieta Sunnyvale Station	0.50	14	Loma Prieta Sunnyvale Station	1.25
6	Loma Prieta Palo Alto Station	0.50	15	Loma Prieta Palo Alto Station	1.25
7	Simulated motion	0.75	16	Loma Prieta Palo Alto Station	1.50
8	Loma Prieta Sunnyvale Station	0.75	17	Loma Prieta Palo Alto Station	1.75
9	Loma Prieta Palo Alto Station	0.75			

In all tests, the applied ground motions were recorded on the table, along with the response accelerations at the center of each of the three floors. Inelastic response was experienced in runs 10-17 as observed by the period elongation in Figure 14, and the buckled coupons in Figure 13d. Predictions were conducted using two training sets. First training set included runs 1-13, with a mix of linear elastic and inelastic responses and predicted the inelastic responses in runs 14-17. The predicted acceleration response at the third floor in run 17 is compared with the recorded response in Figure 15. The prediction is reasonable in the time domain; however, it fails to capture the period elongation in the frequency domain. Although the training set covers the entire range of response, this is an indication that the number of motions in the training set is not sufficient. Accordingly, the number of motions in the second training set was increased to 16 (runs 1-16), while only run 17 was used for testing. Figure 16 shows the improved predictions, where the time history of the predicted acceleration response is close to the true acceleration response and the period elongation is captured. It is also observed that the predicted acceleration response includes the 2nd and 3rd mode natural frequencies in the frequency content, similar to the recorded response.

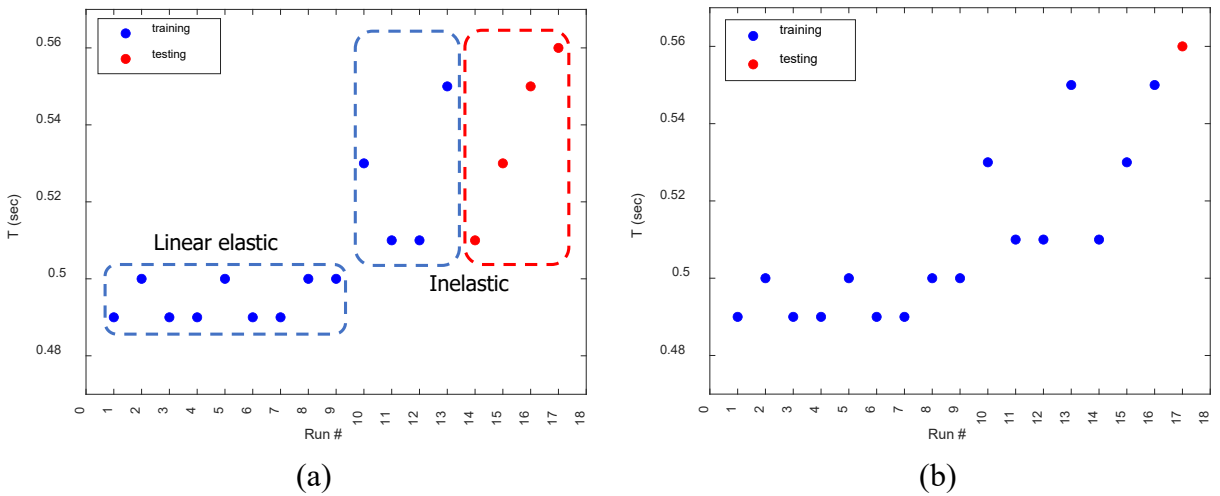


Figure 14. (a) First and (b) second training and testing sets used to predict the acceleration responses of the structure tested on the shaking table.

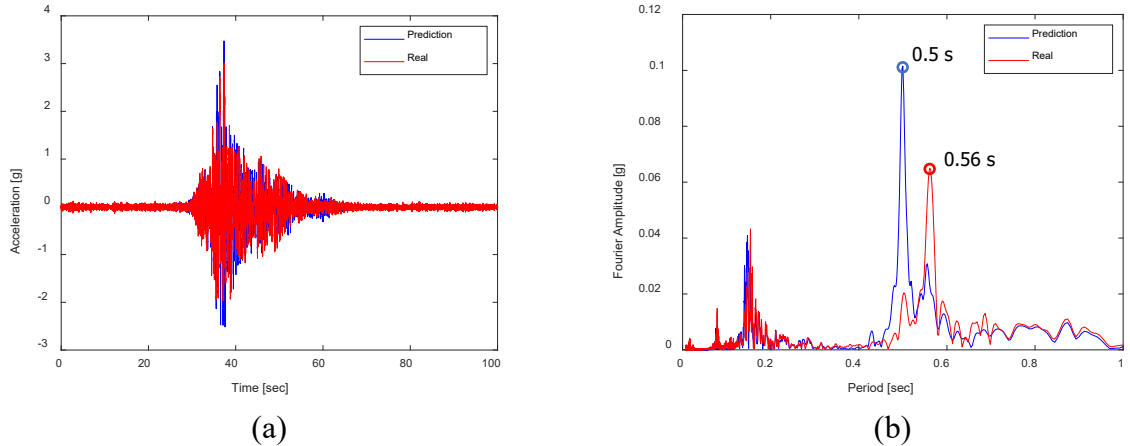


Figure 15. Comparison of (a) time history, (b) frequency content of predicted and recorded accelerations at 3rd floor of tested REPEAT frame (Run 17) [training set with 13 motions].

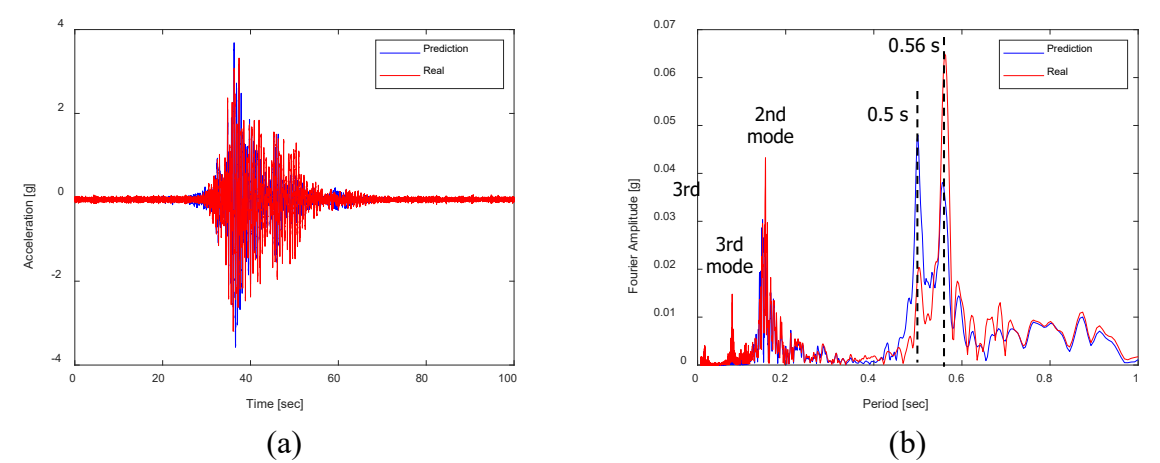


Figure 16. Comparison of (a) time history, (b) frequency content of predicted and recorded accelerations at 3rd floor of tested REPEAT frame (Run 17) [training set with 16 motions].

SDOF Numerical Model

The characteristics of the SDOF system used for prediction of inelastic response is shown in Figure 17a. This SDOF system is developed to be represent low- and mid-rise buildings and has a period of 0.5 s and damping ratio of 5%. Considering a location with design acceleration of 1.0g, Response Modification Factor (R) of 8, and overstrength of 1.6, the yield base shear (F_y) is 20% of the weight W. The force-deformation relationship is bilinear with a strain hardening ratio of 1.0% of initial stiffness. Ninety-three motions with varying intensity levels were selected from the PEER Ground Motion (GM) database, and nonlinear time history analyses were conducted using these 93 motions. From these input – output (i.e., ground motion – computed response acceleration), 83 and 10 time-histories were used for training and testing, respectively. To predict the inelastic response, the training set covers the entire range of linear elastic and inelastic responses, while the testing set includes the analyses with moderate to very high levels of inelastic response, i.e., ductility demands between 6 and 14 (Figure 17b).

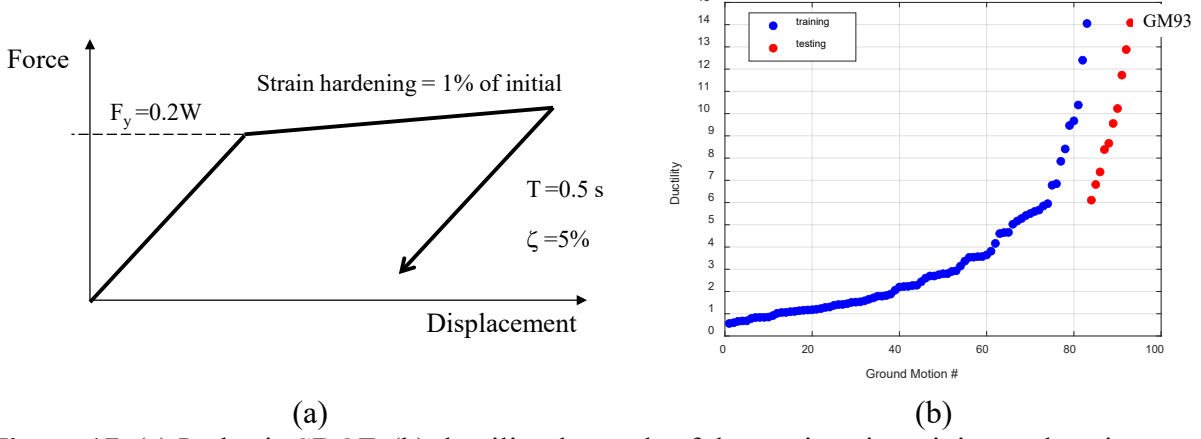


Figure 17. (a) Inelastic SDOF, (b) ductility demands of the motions in training and testing sets.

The prediction results from ground motion GM93 (Figure 17) is shown in Figure 18. The force-displacement relationship in Figure 18e is a highly inelastic response. The pattern of the predicted acceleration matches the true response well, both in the linear elastic and inelastic response ranges. The frequency content and the period elongation are well-captured. The main issue is the overestimated accelerations in the inelastic response range, where the computed acceleration response was capped around 0.25g, which is explained using the following equation of motion of an inelastic SDOF system:

$$ma + cv + f_r = 0, (1)$$

where m is the mass, c is the damping coefficient, and f_r is the restoring force of the SDOF. Because $\zeta=5\%$, the damping force can be ignored, and the maximum acceleration that the SDOF can experience (a_{max}) is expressed as follows:

$$a_{max} = f_{r,max}/m \tag{2}$$

where $f_{r,max}$ is the maximum restoring force. For the highest experienced ductility of 14 (Figure 17b) and strain hardening of 1%, $f_{r,max} = F_y + F_y / \delta_y \times 0.01 \times (14\delta_y - \delta_y) = 1.13F_y = 0.23W$ (Figure 17a), resulting in $a_{max} = 0.23g$, which may further slightly increase because of the damping force.

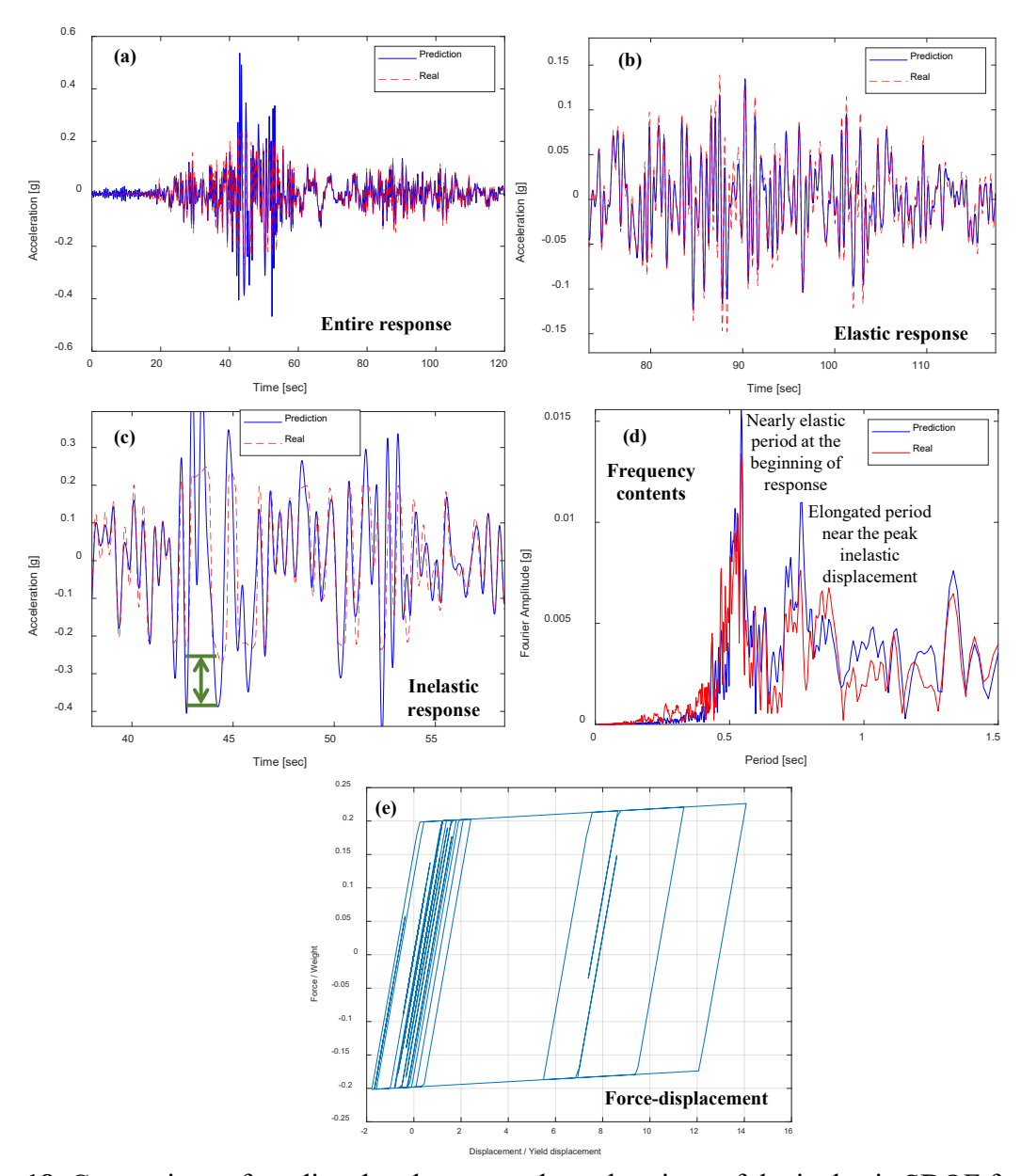


Figure 18. Comparison of predicted and computed accelerations of the inelastic SDOF for GM93: (a) entire response, (b) elastic response, (c) inelastic response, (d) frequency domain, (e) computed force-displacement relationship.

The TCN model was not able to capture this cap with 83 motions in the training set. Instead of increasing the number of motions in the training set, e.g., by an order of magnitude, one possible solution to overcome this limitation is the use of Physics-informed Neural Networks (PINNs) (Raissi et al., 2019; Eshkevari et al., 2021), which received increased attention in recent years. A PINN-based architecture can be thought of as a hybrid modeling approach, which combines the advantages of physics-based and data-driven approaches. The main advantage of a PINN is the ability to use physics-based information to complement the data-driven Artificial Intelligence (AI) model. This information is generally an important local information, e.g., the acceleration cap of the SDOF system, that requires a much larger number of training data

compared to that needed for the AI model to learn global underlying physics. Using PINN, this acceleration cap can be introduced to the TCN model as a constraint, instead of expecting the TCN to learn the presence of this cap using a very large training data set. The integration of PINN into the TCN model is especially important considering that the amount of data with inelastic behavior from instrumented structures is limited. The incorporation of PINNs to the TCN model for overcoming the issue of the acceleration cap is worth exploring in future studies.

Ground Motion Prediction

The successful response predictions discussed in the earlier sections show that the TCN model can capture well the transfer function between the input ground motion and the output acceleration response. Because the ground motion can be calculated using the output acceleration response and the inverse of the transfer function, the TCN model is expected to successfully perform predictions that use the inverse of the transfer function in the reverse case, given the accurate predictions in the forward case. With this expectation, ground motions are predicted from the recorded response accelerations using the TCN model in this section.

The computation of the ground motion from the response is helpful from different perspectives in cases where ground motions are not available. It can facilitate the use of measured response for obtaining the ground motion to characterize the intensity of shaking in regions where ground motion recording stations is scarce. In these locations of scarce ground motion recording stations, the number of conventionally instrumented buildings (e.g., instrumented as part of CSMIP) are even less. However, there are buildings instrumented with alternative means, such as the Community Seismic Network, CSN (Clayton et al. 2015) or apps like MyShake (Kong et al., 2016), which employ smartphone accelerometers and crowdsourcing. Such alternative instrumentation at floor levels can be used to predict the ground motions at locations where the ground motions are not available. The prediction of ground motions can result in other benefits, such as facilitating the use of input-output methods for system identification, which are superior compared to the output-only methods. Ground motions are predicted for the mid-rise and tall buildings discussed in the earlier sections, and these predictions are discussed in the following sections.

6-Story RC Hotel Building in San Bernardino EW Direction

In the earlier section that focused on the prediction of the floor accelerations of the San Bernardino building in the EW direction, Channel 1 on the 1st floor was used as input, and Channel 4 on the 3rd floor was output. In the reverse case to predict the ground motion, Channels 4 and 1 are used as input and output, respectively. The same 10 motions used for response predictions are used in the training set for ground motion predictions. Figure 19 compares the predicted and recorded ground motion acceleration history and the corresponding acceleration response spectra for two events in the testing set. It is observed that the time history and response spectra of the predicted accelerations match those of the recorded ones very well.

Ground motions are commonly characterized with several intensity measures (IMs) for various purposes, such as development of ShakeMaps (Worden et al., 2018) and formulating the fragility functions for use in PBEE (Günay and Mosalam, 2013). Therefore, the various IMs of

predicted and recorded ground motions, including PGA, spectral acceleration (Sa) at 1st mode period, Arias Intensity (Ia), Peak Ground Velocity (PGV), and Cumulative Absolute Velocity (CAV) are compared for all motions in the testing set, Figure 20. The predicted values are very close to the recorded ones, showing that the developed TCN model is capable of predicting the ground motions using the response accelerations of a mid-rise building.

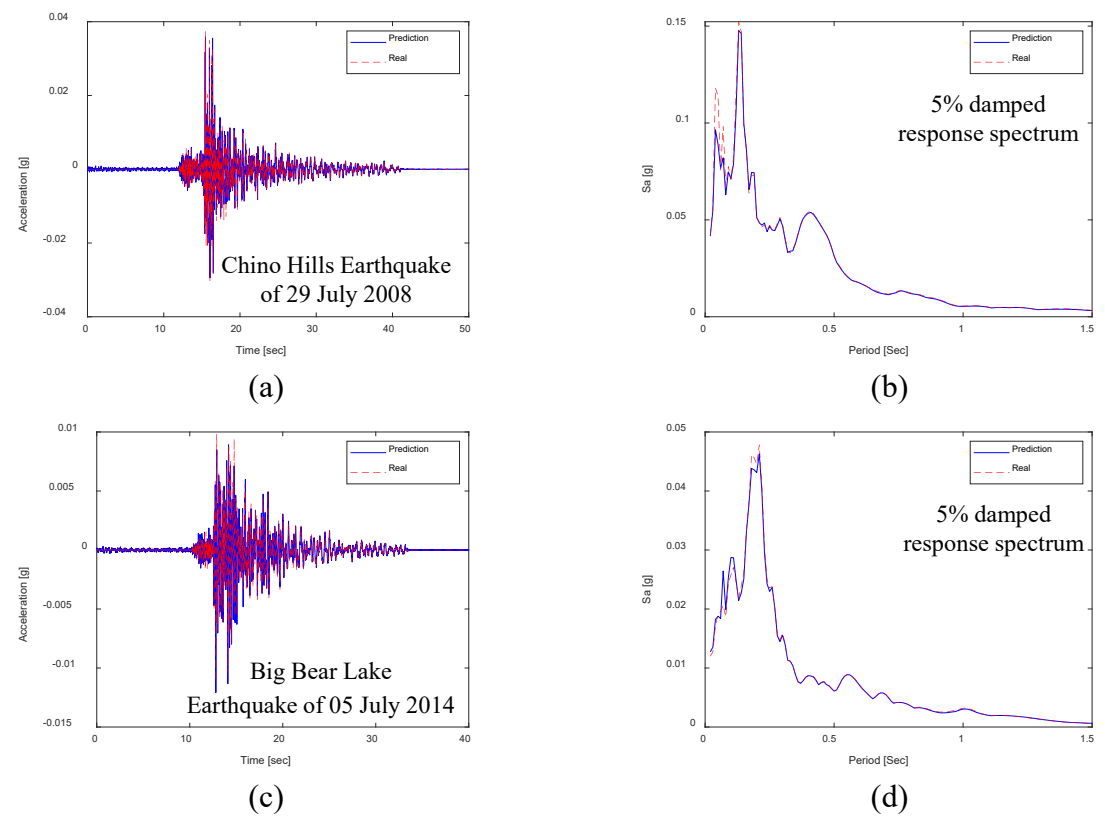


Figure 19. Comparison of the predicted and recorded ground motion (a, c) acceleration time histories, (b, d) 5% damped acceleration response spectra for two of the events in the testing set.

Tall Building with Higher Modes

The difficulty of predicting responses that include higher modes also apply to the ground motion predictions. Therefore, ground motions are predicted for the tall building in this section to evaluate the accuracy of the predictions. The same training and testing sets used for the response predictions are utilized for predicting the ground motions by changing the input and output data. Three different ground motion predictions were performed using three training sets, where in all the sets, the output is the motion at the ground level, while the input in sets 1, 2, 3 are the response acceleration at levels 46, 36, and 20, respectively. The presence of higher modes was expected in all three sets, but with different levels because of the mode shapes and the varying contribution of higher modes at different floors. As observed in Figure 21, the predicted ground motion time histories are close to the recorded ones, but not as close as the predictions for the San Bernardino building with the first mode building response. These differences between the predictions and recorded ground motions are more clearly observed in the acceleration response spectra. Using observations from San Bernardino building and the tall

building, it is concluded that ground motion predictions are accurate using response governed by first mode, and more training data is needed for successful predictions involving higher modes or inelastic effects. However, it was not possible to explore how many more motions are needed in the training set for accurate predictions, because all the events recorded for this building are already used and no additional data is available. This highlights the need for increased instrumentation of buildings and bridges.

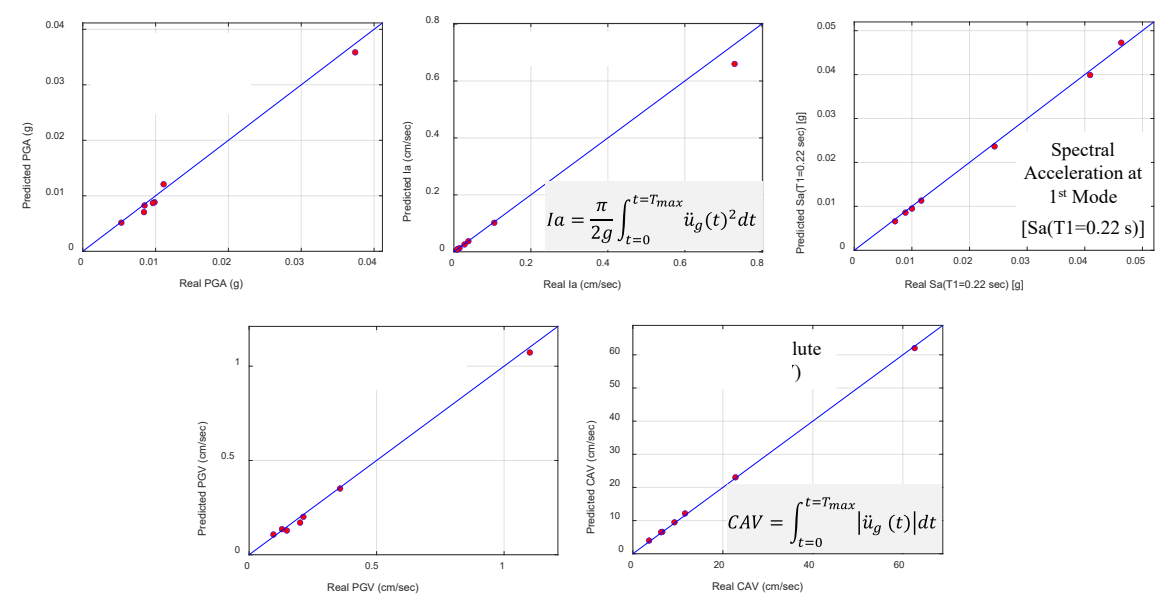


Figure 20. Comparison of predicted and recorded IMs for all motions in the testing set.

Summary, Conclusions, and Future Directions

This paper focused on the use of Temporal Convolutional Network (TCN) models for determining the structural response in the form of time histories. Models were trained using the data from several structural systems with different characteristics to predict the response. The results were explained using concepts of structural dynamics and applications in earthquake engineering. Table 4 provides a summary of the predictions for the studied structural systems. This table shows that the developed TCN model is successful in predicting the responses of the numerical models, shaking table tested structure, and several instrumented buildings, which span a broad range of response characteristics, using a practical number of motions for training in most of the cases. The limitations of the current methodology are identified, such as the issues with predicting the capped accelerations of the inelastic SDOF system, which can be resolved in future studies with recent advances in Artificial Intelligence (AI) models that make use of the physics-based information.

Acknowledgements

This research is supported by the California Department of Conservation, California Geological Survey, Strong Motion Instrumentation Program agreement 1022-002.

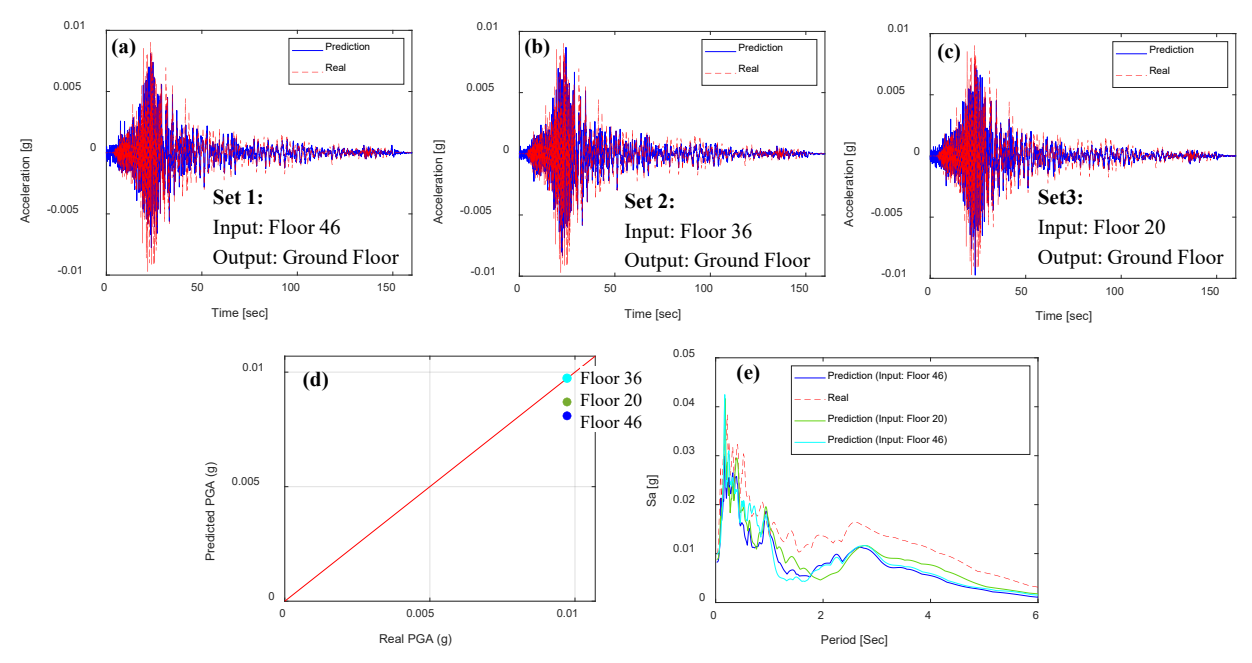


Figure 21. Comparison of predicted and recorded ground motion (a, b, c) acceleration time histories, (d) PGA, (e) 5% damped acceleration response spectra for the event in the testing set.

Table 4. Summary of the TCN model predictions for different structural systems

Table 4. Summary of the Ten model predictions for different structural systems					
Prediction Type	System	# of motions in the training set	Quality of the predictions		
Linear	SDOF	7	Successful		
elastic	Two instrumented low- & midrise buildings	10	Successful		
response	Instrumented tall building	10	Successful		
Inelastic	Bilinear SDOF	83	Partially successful, needs PINNs for improving peak response		
response	3-story SMRF tested on the shaking table	13 / 16	Needs improvement / Successful		
	Instrumented mid-rise building	10 / 23	Needs improvement / Successful		
Ground	Instrumented mid-rise building	10	Successful		
motion	Instrumented tall building	10	Successful, predictions can be improved with more data		

References

Brownjohn, J.M.W., Au, S.K., Zhu, Y., Sun, Z., Li, B., Bassitt, J., Hudson, E., and Sun, H., 2018. Bayesian operational modal analysis of Jiangyin Yangtze River bridge. *Mechanical Systems and Signal Processing*, 110, 210-230.

Chen, Y., Sun, Z., Zhang, R., Yao, L., and Wu, G., 2023. Attention mechanism based neural networks for structural post-earthquake damage state prediction and rapid fragility analysis. *Computers & Structures*, 281, 107038.

Chopra, A.K., 2017. Dynamics of Structures, Theory and Applications to Earthquake Engineering, 5th Edition. Hoboken, NJ, Pearson Education, 960.

- Clayton, R.W., Heaton, T., Kohler, M., Chandy, M., Guy, R., and Bunn, J., 2015. Community seismic network: A dense array to sense earthquake strong motion. *Seismological Research Letters*, 86(5), 1354-1363.
- Cruz, C. and Miranda, E., 2017. Evaluation of damping ratios for the seismic analysis of tall buildings. *Journal of Structural Engineering*, 143(1), 04016144.
- Eshkevari, S.S., Takáč, M., Pakzad, S.N., and Jahani, M., 2021. DynNet: Physics-based neural architecture design for nonlinear structural response modeling and prediction. *Engineering Structures*, 229, 111582.
- Günay, S. and Mosalam, K.M., 2013. PEER performance-based earthquake engineering methodology, revisited. *Journal of Earthquake Engineering*, 17(6), 829-858.
- Günay, S., Pang, I.K.T., and Mosalam, K.M. (2023) Structural Response Prediction Using Deep Neural Networks. Proceedings of SMIP2023.
- Kong, Q., Allen, R.M., Schreier, L., & Kwon, Y.W. (2016). MyShake: A smartphone seismic network for earthquake early warning and beyond. *Science advances*, 2(2), e150105.
- Kundu, A. and Chakraborty, S., 2020, September. Deep learning-based metamodeling technique for nonlinear seismic response quantification. In IOP Conference Series: Materials Science and Engineering (Vol. 936, No. 1, p. 012042). IOP Publishing.
- Lea, C., Flynn, M.D., Vidal, R., Reiter, A., and Hager, G.D., 2017. Temporal convolutional networks for action segmentation and detection. In proceedings of the IEEE Conference on Computer Vision and Pattern Recognition, 156-165.
- Li, B. and Spence, S.M., 2022. Metamodeling through deep learning of high-dimensional dynamic nonlinear systems driven by general stochastic excitation. *Journal of Structural Engineering*, 148(11), 04022186.
- McCallen, D., Petersson, A., Rodgers, A., Pitarka, A., Miah, M., Petrone, F., Abrahamson, N., and Tang, H., 2021. EQSIM—A Multidisciplinary Framework for Fault-to-Structure Earthquake Simulations on Exascale Computers Part I: Computational Models and Workflow. *Earthquake Spectra*, 37(2), 707-735. doi:10.1177/8755293020970982.
- Muin, S. and Mosalam, K.M., 2018. Localized Damage Detection of CSMIP Instrumented Buildings using Cumulative Absolute Velocity: A Machine Learning Approach. In Proceedings of the SMIP18 Seminar on Utilization of Strong-Motion Data, Sacramento, CA, USA (Vol. 25).
- Muin, S. and Mosalam, K.M., 2017. Cumulative absolute velocity as a local damage indicator of instrumented structures. *Earthquake Spectra*, 33(2), 641-664.
- Park, Y.J. and Ang, A.H.S., 1985. Mechanistic seismic damage model for reinforced concrete. Journal of Structural Engineering, 111(4), 722-739.
- Park, Y.J., Ang, A.H.S., and Wen, Y.K., 1985. Seismic damage analysis of reinforced concrete buildings. *Journal of Structural Engineering*, 111(4), 740-757.
- Raissi, M., Perdikaris, P., and Karniadakis, G.E., 2019. Physics-informed neural networks: A deep learning framework for solving forward and inverse problems involving nonlinear partial differential equations. *Journal of Computational Physics*, 378, 686-707.
- Worden, C.B., Hearne, M., and Thompson, E.M., 2018. ShakeMap v4 Software, USGS Software Release. https://doi.org/10.5066/P97FHE0I.
- Zhang, R., Chen, Z., Chen, S., Zheng, J., Büyüköztürk, O., and Sun, H., 2019. Deep long short-term memory networks for nonlinear structural seismic response prediction. *Computers & Structures*, 220, 55-68.
- Zhong, K., Navarro, J.G., Govindjee, S., and Deierlein, G.G., 2023. Surrogate modeling of structural seismic response using probabilistic learning on manifolds. *Earthquake Engineering & Structural Dynamics*, 52(8), 2407-2428.